



The importance of alpine blowing snow for cloud processes

Samuele Viaro¹, Armin Sigmund^{1,2}, Evan Thomas¹, and Michael Lehning^{1,3}

¹Ecole Polytechnique Fédérale de Lausanne. Rte des Ronquos 86, 1950 Sion, Switzerland

²University of Basel. Peterspl. 1, 4001 Basel, Switzerland

³WSL Swiss Federal Institute for Snow and Avalanche Research. Flüelastrasse 11, 7260 Davos, Switzerland

Correspondence: Samuele Viaro (samuele.viaro@epfl.ch)

Abstract. Numerical models are known to fail in reproducing the large gap that exists between measured ice nucleating particles and ice crystal number concentrations in alpine regions. Improvements have been made by adding different sources of secondary ice production mechanisms into the models. Blowing snow has been identified as an additional possible source of ice particles. Driven by this assumption, we investigate the effect of blowing snow particles using the numerical model CRYOWRF, in which a new saltation scheme has been implemented to better represent the boundary conditions necessary for the blowing snow equations. First, ice crystal number concentrations are compared with measured data from Jungfrauoch, in the Swiss Alps, showing the importance of secondary ice production, blowing snow and microphysics scheme. Then, erosion and deposition patterns are also analyzed, as well as the influence of blowing snow on precipitation. It is shown that our implementation of blowing snow dynamics improves significantly the match between observed and simulated cloud particles.

1 Introduction

In the domain of cloud physics it is still uncertain why measured ice crystal number concentration (ICNC), with median values around 100 L^{-1} (Mignani et al., 2019), can exceed the concentration of ice nucleating particles (INP) by orders of magnitude, reaching peak levels of more than 1000 L^{-1} in particular conditions. Model simulations usually underestimate ICNC compared with observations. One explanation is that primary ice production alone is insufficient to reproduce the ICNC (Georgakaki et al., 2022). The Hallett–Mossop process (Hallett and Mossop, 1974) is a powerful secondary ice production (SIP) mechanism implemented in most atmospheric models, but it is only active in the temperature range $-8^\circ\text{C} < T < -3^\circ\text{C}$. Korolev et al. (2022) performed measurements on an aircraft cruising at approximately 6500 m at -27°C to analyze six different secondary ice production mechanisms in the attempt to explain values of ICNC above 1000 L^{-1} . They concluded that no dominating mechanism could be identified, and speculated on an unknown mechanism to explain such high values. Blowing snow (BS) is believed to be one of the causes affecting this discrepancy (Geerts et al., 2015) but its influence on ICNC remains poorly understood. Since secondary ice production requires the prior presence of other ice particles (Vali, 1985), BS can indeed contribute to create both additional particles and collisions that could consequently produce more ice crystals. Georgakaki et al. (2022) attempted to investigate this by including a constant source of BS particles at the first model level in their simulations, suggesting the importance of combining BS and SIP. More recent studies (Sotiropoulou et al., 2024; Georgakaki et al., 2024) restated that advanced blowing snow models could be beneficial to reduce the uncertainties associated with the estimation



of ICNC. This prompted us to use the model CRYOWRF (Sharma et al., 2023), which has at its core the Weather Research and Forecasting (WRF) atmospheric model. Blowing snow particles are modelled with a double-moment scheme that solves prognostic equations for the mass and number mixing ratios. It is well known that the wind speed needed to dislodge particles from the surface and transport them via turbulent motions depends on the condition of the surface snow (Mellor, 1965; Schmidt, 1982a), e.g., wind speed of 3 to 8 m s⁻¹ will suffice only for loose and unbounded snow. In CRYOWRF, the land surface model implemented is SNOWPACK (Lehning et al., 1999) which accurately predicts snow surface conditions, critical for modelling blowing snow dynamics. Validation of the CRYOWRF model is achieved through observational data from the Cloud and Aerosol Characterization Experiment (CLAVE) 2014 campaign at Jungfraujoch (Lloyd et al., 2015).

The importance of modelling blowing snow is not limited to properly estimating the ICNC. The effect of wind on redistribution during and after precipitation events is an important driver for the mass balance of alpine regions and a prerequisite for reliably estimating avalanche danger. This snow transport considers particles that either fall from above through precipitation, leading to preferential deposition (Lehning et al., 2008), or are picked up from the surface whenever a threshold velocity is reached (Mellor, 1965). Lehning and Fierz (2008) assessed transported snow using local meteorological measurements from atmospheric weather stations and the SNOWPACK model. In another study, the three-dimensional effect of blowing snow on wind-induced snow transport was numerically investigated at a high horizontal resolution of 50 m, showing changes in deposition patterns when blowing snow effects were neglected (Vionnet et al., 2014). With a sensitivity analysis on model resolution, Gerber et al. (2019) showed that 50 m horizontal grid spacing is necessary to capture leeside flow separations that affect snow redistribution and precipitation processes. Acknowledging that the redistribution of snow by wind modifies the variability in the accumulation of snow in both alpine terrains and polar regions, Saigger et al. (2024) recently implemented blowing snow equations in WRF focusing on a computationally efficient module and highlighting the necessity of including blowing snow within atmospheric models. On a larger temporal scale, models like MAR can be a valuable tool for a realistic representation of snow cover variability in alpine regions at relatively low resolution (Beaumet et al., 2021). Blowing snow also plays an important role in the surface mass balance of Antarctica, where van Dalum et al. (2025) demonstrated the importance of correctly parameterizing this phenomenon both in terms of transport and sublimation.

One final motivation to account for BS in numerical models comes from the concept that complex interactions of fluid dynamics and thermodynamics mechanisms, driven by surface orography, subsequently influence cloud microphysical processes that define patterns of precipitation (Roe, 2005). Knowing that in midlatitudes and polar regions precipitation events are either snow or rain formed from melting snow (Field and Heymsfield, 2015), and that blowing snow particles do reach cloud levels (Bergner et al., 2025), assessing how BS interacts with microphysical processes to modify precipitation is highly important. This is particularly true since, given the necessary conditions, blowing snow particles could sublimate, leading to a change in the atmospheric moisture, temperature and stability. In CRYOWRF, the effect of blowing snow sublimation is accounted for in the prognostic equations.

This paper focuses on showing the importance of BS modeling in correctly reproducing ICNC, snow transport and precipitation. The structure of the paper is as follows. Methodology is described in Sect. 2 including the numerical models used, measured data and recent updates on CRYOWRF. Results are shown in Sect. 3, in which we first analyze the influence of



primary ice production, secondary ice production and blowing snow on ICNC, and then show snow transport and precipitation patterns.

2 Methodology

The methodology involves a numerical analysis of the test site using observational data as validation.

65 2.1 Measured data

Experiments were performed at the high-alpine Sphinx laboratory of Jungfrauoch (JFJ) located 46.55°N, 7.89°E on a saddle between two mountain peaks in the Bernese Alps, Switzerland, surrounded by glaciers and rocks. With an altitude of 3454 m, it is the highest European railway station, easily accessible throughout the year. Due to its topography, shown in Fig. 1, winds are constrained in two main directions, which approximately align with the cross section A-A'. Air coming from the northwest faces steep terrains whereas for southeasterly winds the Aletsch Glacier offers more gentle slopes. Baltensperger et al. (1998) reported an annual mean cloud frequency of 37% at the site, making it a suitable location for the study of long-term cloud microphysical properties of supercooled clouds in this region. An overview of the instrumentation used to derive the measurements data used in this paper can be found in Lloyd et al. (2015) and Grazioli et al. (2015).

2.2 Numerical models

75 The numerical non-hydrostatic models used in this paper are WRF v4.7.1 and CRYOWRF v1.2.2. They use a configuration with three two-way nested domains that cover the geographical area shown in Fig. 2, centered at JFJ. Domains d01, d02, d03 have a horizontal resolution of 9, 3, 1 km respectively, allowing for the resolution of cloud microphysics in the innermost domain. The parent domain consists of 121 x 121 grid points, whereas the other two domains use 151 x 151 grid points each. The Lambert conformal conic projection was used to map the domain, given its effectiveness for regional weather models over mid-latitudes. The model top is set at 5000 Pa, corresponding to 20 km circa, with 100 vertical levels and a 1.1 stretch. The case study considered starts on 25 January at 00:00 and ends on 28 January at 00:00. All timestamps are reported in UTC for the 2014 calendar year. The spinup time was chosen to be of 24 hours with timesteps of 27, 9 and 3 s for the first, second and third domain, respectively. The ERA5 global reanalysis dataset (Hersbach et al., 2020), with a resolution of 0.25x0.25°, provides the initial conditions as well as the lateral forcings every hour. The WRF pre-processing system is used for the static data. MODIS 85 15s land use categories define the two coarser domains, whereas the inner-most domain uses Copernicus 3s. Short-wave and long-wave radiation are parametrized with the RRTGM scheme. The fine grid of domain d03 allows to resolve cumulus-type clouds, which are parametrized in domain d01 and d02 with the Kain-Fritsch parametrization scheme. The ISHMAEL (Jensen et al., 2017) and the Morrison double-moment scheme (Morrison et al., 2009), from now on MOR, were selected for resolving cloud and precipitation processes. The latter is modified in CRYOWRF to include SIP processes. The grid resolution is not fine 90 enough to resolve the planetary boundary layer, which is instead parametrized with the turbulent kinetic energy scheme Mellor-Yamada Janjic coupled with the Eta Similarity surface layer scheme. The land surface model switches from Noah-MP (Niu

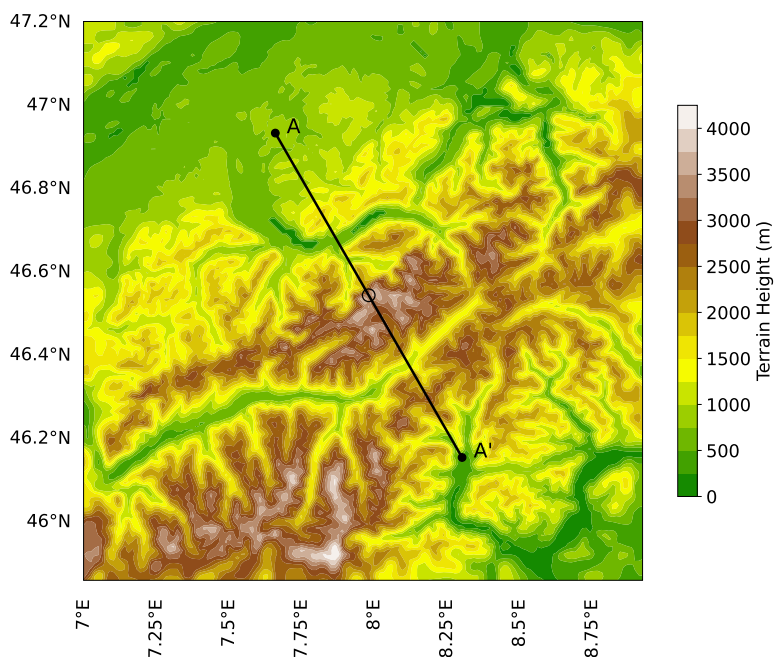


Figure 1. Topography of the region surrounding JFJ derived from the innermost domain d03. The open black circle indicates JFJ. Cross section A-A' centered at JFJ. A color-blind version is provided in the supplementary material as Fig. S1.

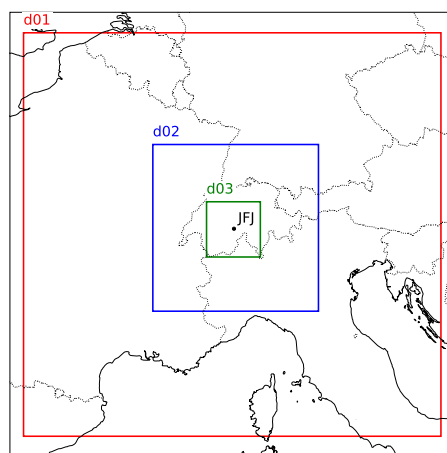


Figure 2. The three nested domains of the simulations, centered at JFJ.

et al., 2011; Yang et al., 2011) for the WRF simulations, to SNOWPACK for the CRYOWRF simulations. All results shown are for the innermost domain d03. Table 1 summarizes the main parameters changed during the simulations. The reference



Table 1. Details of the models and schemes for each simulation ID.

ID	Land Surface Model	Microphysics	Blowing Snow	Secondary Ice Production	Model
CTRL	Noah-MP	Morrison	N	-	WRF v4.7.1
ISH	Noah-MP	ISHMAEL	N	-	WRF v4.7.1
MOR_BS	SNOWPACK	Morrison	Y	BR300	CRYOWRF v1.2.2
MOR_noBSeq	SNOWPACK	Morrison	N	BR300	CRYOWRF v1.2.2
MOR_BSortig	SNOWPACK	Morrison	Y	BR300	CRYOWRF v1.0.0
ISH_BS	SNOWPACK	ISHMAEL	Y	-	CRYOWRF v1.2.2

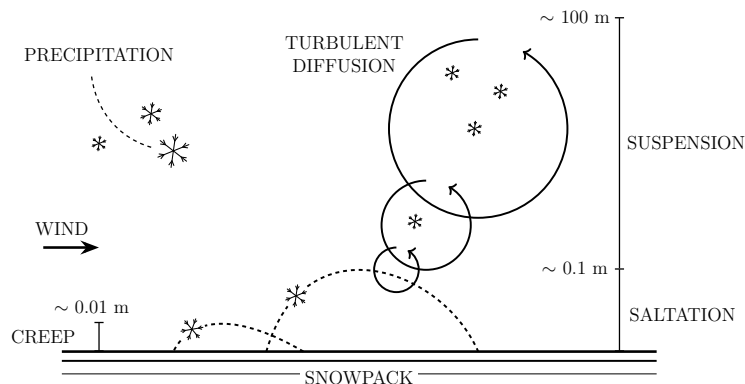


Figure 3. Snow transport processes sketch showing the differences between creep, saltation and suspension.

case considered (CTRL) involves the WRF model, Noah-MP, MOR, without blowing snow equations nor SIP. In two of the
 95 CRYOWRF simulations (MOR_BS, MOR_BSortig), we use the SIP scheme named BR300 and explained in Sect. 2.2.1.

2.2.1 CRYOWRF simulations

Ice particles that collide with each other are a known source of ice multiplication through mechanical breakup (BR). Hoarau
 et al. (2018) implemented this process into a mesoscale model by assuming constant number of fragments per collision between
 snow and graupel exclusively. CRYOWRF includes the extended version of this process which neglects solely the collision
 100 between small ice particles, i.e. cloud ice, and considers the other type of collisions between snow-graupel-ice, resulting in
 a more realistic approach. This SIP scheme (BR300) was added to the standard MOR, and allows ice multiplication only if
 the particle is larger than a threshold set to 300 μm . Particle collisions are assumed to generate one fragment. Details of the
 implementation and equations can be found in Appendix B of Sotiropoulou et al. (2020).

Increasing the intensity of the flow near the surface, turbulent even in light breezes, causes snow particles to roll, jump or
 105 being lifted by turbulent eddies through processes named creep, saltation or suspension, respectively (Fig. 3). Snow particles



are modelled with a double-moment scheme that solves prognostic equations for the mass and number mixing ratio. Blowing snow is highly governed by grain size and cohesion, information that is available through the coupling between the atmospheric model WRF and the land surface model SNOWPACK. Saltation, which happens within ≈ 10 cm from the surface, is parametrized and acts as the lower boundary condition for the blowing snow equations. Details of the implementation of blowing snow in CRYOWRF can be found in Sharma et al. (2023).

2.2.2 CRYOWRF updates

In CRYOWRF v1.2.2, the saltation scheme was modified to better estimate the lower boundary conditions for the prognostic equations for blowing snow. These lower boundary conditions are defined at the interface between the saltation layer and suspension layer. In the previous model version, the height of this interface was computed using the friction velocity dependent parametrization of Pomeroy and Male (1992). However, this parameterization underestimated the height of the saltation-suspension interface and thus contributed to an overestimation of the mass and number mixing ratios of blowing snow at greater heights, compared to large-eddy simulations with Lagrangian snow particles (Sigmund et al., 2025; Melo et al., 2022). In CRYOWRF v1.2.2, we therefore prescribe an interface height of 0.15 m, which is consistent with splash dominated saltation (Melo et al., 2024). Due to this relatively high value, we reduce the mean particle diameter at this height from 200 μm to 140 μm , which is in the range of values (approximately 80 to 160 μm) reported for a height of 0.15 m in the literature (Nishimura and Nemoto, 2005; Schmidt, 1982b). The horizontal particle speed at the interface height was previously assumed to be proportional to the threshold friction velocity for snow transport and independent of wind speed. As this assumption is only appropriate in the lowest 3 cm of the saltation layer (Melo et al., 2024), we assume the horizontal particle speed at the interface height to be 75% of the wind speed, which is in line with measurements of Nishimura et al. (2014). CRYOWRF computes an exponential vertical profile for the horizontal saltation mass flux following (Nishimura and Hunt, 2000). The decay height parameter of this profile is a quadratic function of friction velocity. However, large-eddy simulations with Lagrangian snow particles suggest that this parameter becomes nearly independent of friction velocity at high friction velocities (Melo et al., 2024). Therefore, we introduce an upper limit of 4 cm for the decay height parameter, which is based on Fig. 4 in Melo et al. (2024). This modification reduces the blowing snow mixing ratios at the interface height for high friction velocities. In the suspension scheme, we improve the vertical resolution near the surface by using stretched vertical grid levels in the fine mesh with a logarithmic instead of equal spacing. This improvement helps to better resolve the strong vertical gradients of the blowing snow mixing ratios near the surface and thus avoids a strong overestimation of snow transport (Sigmund et al., 2025). To mitigate the remaining overestimation caused by insufficient vertical resolution, we modify the discretization of the sedimentation term in the prognostic equations for blowing snow, as proposed by Sigmund et al. (2025). More precisely, this term is expressed using forward finite differences for the blowing snow mixing ratios and backward finite differences for the terminal fall velocities.

The structure of the repository was also updated. The original CRYOWRF v1.0.0 repository, developed by Sharma et al. (2023), contained the external repositories of WRF, WRF Preprocessing System (WPS), SNOWPACK and MeteorIO directly embedded, along with the coupler. In order to keep track of version control histories for each repository, we deleted the

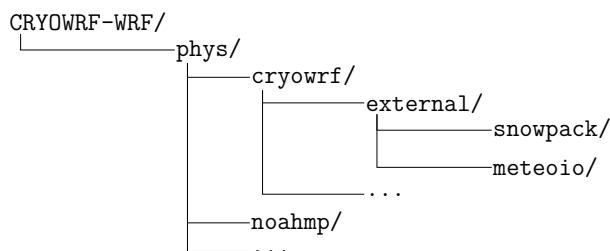


Figure 4. Structure of the repository CRYOWRF-WRF.

140 WRF and WPS directories and integrated the resulting lightweight CRYOWRF repository into our fork of WRF (CRYOWRF-
WRF) as a submodule, following the same pattern used for integrating Noah-MP, the standard land surface model of WRF.
The updated CRYOWRF only contains the coupler functions as well as SNOWPACK and MeteoIO as external submodule
repositories. The reasoning behind this is that the coupler represents the interface between SNOWPACK, MeteoIO and WRF,
and therefore defines the fixed versions of these dependencies. Work was undertaken to determine the point in time where
145 the SNOWPACK and MeteoIO libraries had been split from their upstream sources, and to coordinate them as submodules
inside the fork keeping the changes from the original versions. In addition, the WRF base version was incremented from v4.2.1
to v4.7.1 while reapplying the initial CRYOWRF physics enhancements in terms of blowing snow, saltation and secondary
ice production, resulting in version v1.2.0. The work for versions v1.2.1 and v1.2.2 was to include contributions from other
development branches, including a revised saltation parameterization (described above). From the perspective of the WRF
150 build system, the structure is described in Fig. 4. A separate fork for WPS (CRYOWRF-WPS) also exists in our repository to
manage the pre-processing. Overall, the structure has become more complex, and makes development on the coupler alongside
its dependencies more challenging. However, we are now able to bring in external changes from all four upstream repositories
(WRF, WPS, SNOWPACK and MeteoIO), and have the possibility of pushing changes back to these projects should we wish
to do so in the future.

155 3 Results

Throughout the paper, snow, graupel and ice crystals are summed to compute ICNC, i.e. number concentration, and ice water
concentration (IWC), i.e. mass mixing ratio. Blowing snow particles are additionally added when considered. Rain and cloud
water mixing ratios constitute the liquid water concentration (LWC). The temporal evolution of ICNC, IWC and LWC is taken
at the first model level at ~ 10 m a.g.l. from the grid cell closest to JFJ. Blue dotted lines are the CTRL simulations. In
160 the microphysics plots, green lines represent the influence of the microphysics scheme while in the secondary ice production
plots black lines represent the influence of the SIP. In both cases, the contribution of blowing snow particles are shown with a
continuous line. Orange dash-dotted lines represent a simulation with the original saltation scheme implemented in CRYOWRF
v1.0.0. Unless otherwise specified, the CRYOWRF simulations were performed with the new saltation scheme.



Given the importance of turbulence in both blowing snow and break up mechanisms, a sensitivity analysis involving the
165 parametrization of the planetary boundary layer was made. The test involved the Yonsei University (YSU) and the Mellor-
Yamada-Janjic (MYJ) schemes, which are respectively associated with the Revised MM5 and Eta Similarity surface layer
schemes (the latter based on Monin-Obukhov theory). For this comparison the thickness of the lowest layer, surface stretch and
number of vertical levels were slightly modified to avoid instability issues. No significant difference were noticed between the
two schemes in the data plotted (not shown), and the MYJ was chosen for this paper.

170 3.1 Meteorological data

Figure 5 shows meteorological parameters compared with observations. Wind velocity and wind direction are plotted at 10 m
above the ground, the former representing the module in the horizontal direction, which is directly related to blowing snow and
computed as:

$$WS_{10m} = \sqrt{U_{10}^2 + V_{10}^2}, \quad (1)$$

175 where U_{10} and V_{10} are the x-wind and y-wind velocity components. Temperature and relative humidity with respect to water
are plotted at 2 m above ground. All simulations show a similar trend, and agree well with observation. Correctly resolving
these variables is crucial: temperature affects the secondary ice production processes, wind speed and direction are directly
related to blowing snow and redistribution (Mott et al., 2014), and increased relative humidity enhances precipitation (Gerber
et al., 2019).

180 Reynolds et al. (2024a) showed that both turbulent flow features and variables crucial for land-surface modeling, e.g. tem-
perature and incoming radiation, are also well represented by HICAR, an intermediate complexity atmospheric model that
benefits from its fast dynamic downscaling compared to traditional atmospheric models.

3.2 Primary ice production

We check the influence of primary ice production by comparing two standard microphysics schemes implemented in WRF,
185 the MOR and ISHMAEL. The latter in particular is highly advanced in predicting the evolution of ice habits and density at the
cost of being slightly more computationally expensive than the former. Note that the MOR scheme in WRF does not include
the breakup SIP which is only present in CRYOWRF. Figure 6 shows that even though the ISHMAEL scheme does not include
particular SIP mechanisms, there is nearly an order of magnitude improvement in ICNC prediction and also a better repre-
sentation of IWC. These results solidify the conclusions of Sotiropoulou et al. (2024), which showed that changing primary
190 ice production treatment in models does strongly impact cloud characteristics. Using an intermediate complexity model, the
two microphysics schemes here investigated, MOR and ISHMAEL, were also compared, showing an outperformance of the
latter over the former in terms of preferential deposition (Reynolds et al., 2024b) and meteorological variables (Reynolds et al.,
2024a). Results from a simulation in which blowing snow equations are active and adding blowing snow particles to the count,
demonstrate a significant improvement especially in regions of strong winds. It is important to point out that including a SIP

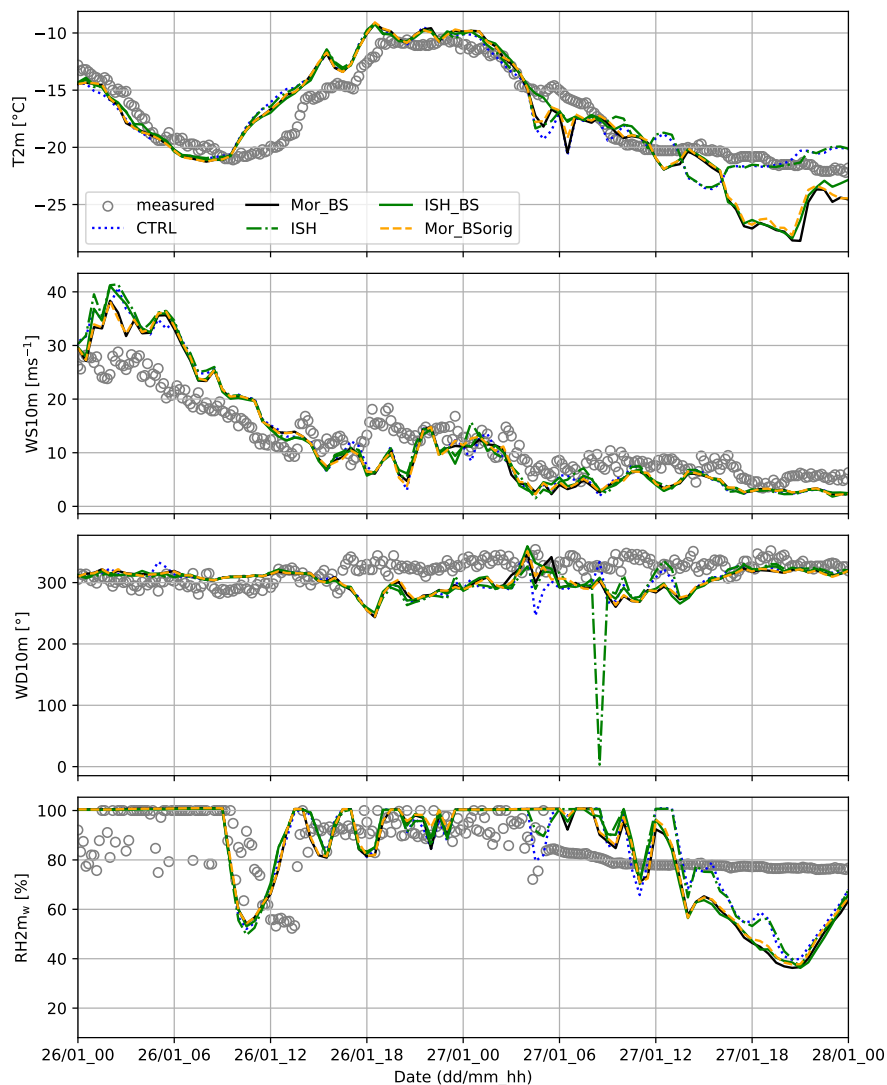


Figure 5. Meteorological data for all simulations. Plots show, from top to bottom, temperature at 2 m, wind speed at 10 m, wind direction at 10 m and relative humidity with respect to water at 2 m.

195 collision break up mechanism in the ISHMAEL scheme could help to fill the gaps of ICNC especially in the region of lower wind speed.

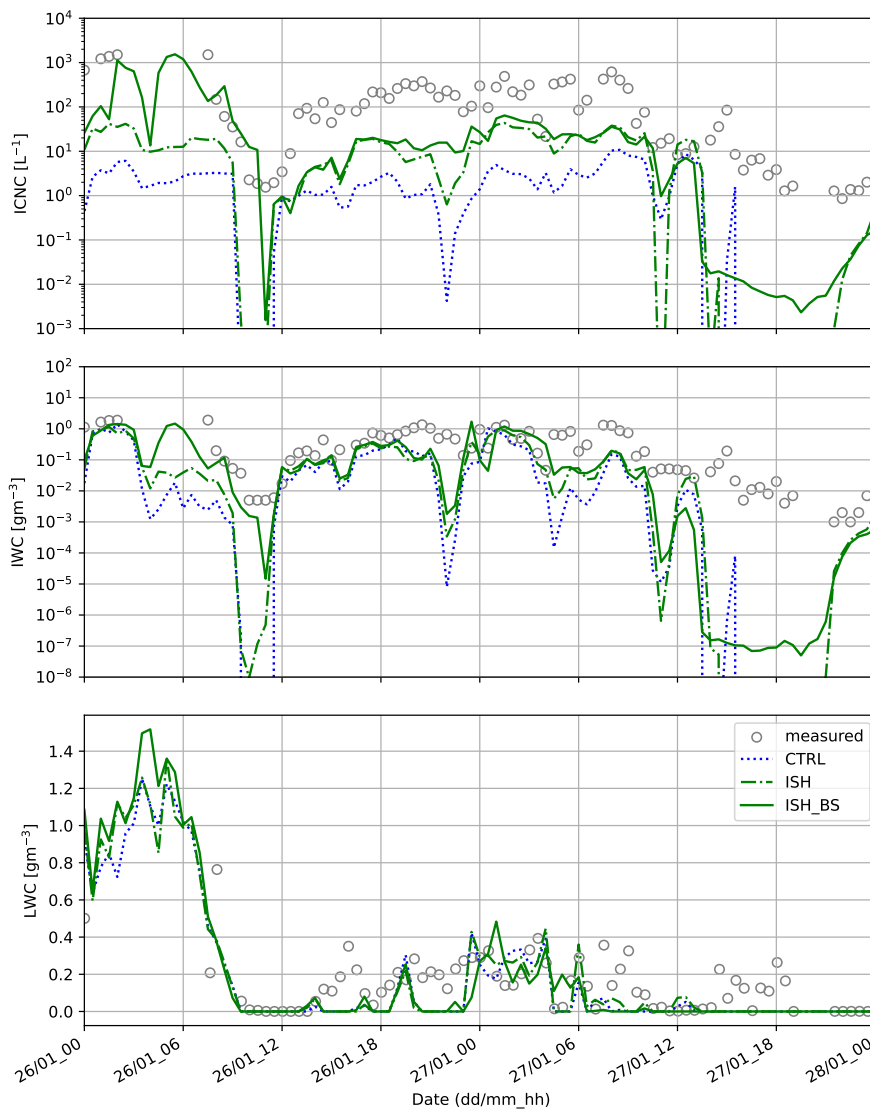


Figure 6. Analyzing the influence of ISHMAEL microphysics scheme and blowing snow particles compared to the CTRL simulation with the Morrison microphysics scheme. Plots show, from top to bottom, ice crystal number concentration, ice water concentration and liquid water concentration.

3.3 Secondary ice production

We use CRYOWRF to test the influence of SIP through the collision break up mechanism that considers a constant number of fragments per collision (Hoarau et al., 2018). It operates in a wider range of temperatures, with maximum efficiency around -16 °C (Takahashi and Nagao, 1995), compared to the classical Hallet-Mossop process implemented in numerical models, which



is effective between $-8\text{ }^{\circ}\text{C}$ and $-3\text{ }^{\circ}\text{C}$. Sotiropoulou et al. (2020) demonstrated that this model tends to overestimate ICNC when all particle sizes are considered per collision, generating one fragment per collision type. The same model underestimates ICNC when ice multiplication is allowed only when particle sizes are larger than $300\text{ }\mu\text{m}$. We performed a sensitivity analysis shifting this threshold to $230\text{ }\mu\text{m}$ which did not show any significant changes in the variables considered. Decreasing it to $130\text{ }\mu\text{m}$ showed a small increase of particle counts (not shown). The SIP with a $300\text{ }\mu\text{m}$ threshold is here implemented into MOR, the standard Morrison scheme of WRF (Morrison et al., 2009).

It can be seen from Fig. 7 that the ICNC measured for temperature around $-15\text{ }^{\circ}\text{C}$ reaches peak values greater than 1000 L^{-1} which are up to three orders of magnitude higher than the predicted primary ice nucleation. Compared to CTRL, including the SIP in MOR (MOR_noBS) improves the ICNC during some time windows investigated, confirming the importance of adding SIP into the estimation of the total ICNC, as shown by Georgakaki et al. (2022). MOR_noBS is the same simulation as MOR_BS where the BS particles are not counted but the blowing snow equations are activated. A sensitivity test in which blowing snow equations are turned off (not shown) shows no difference compared to the MOR_noBS case. In the time window around 27 January at 00:00, this simplified model of SIP does already estimate values of ICNC and IWC in close agreement with measured data, suggesting a strong influence of this process. In terms of the IWC and LWC there are no significant changes, the latter in particular having overlapping values. When the blowing snow particles are added to the count of ICNC and IWC (MOR_BS) there is a significant improvement of the results, particularly in the two time windows of velocities stronger than 10 m s^{-1} . In addition, the two time periods where CTRL fails to predict any particles are now partially filled by the presence of blowing snow particles. In the region of $\text{ICNC} > 1000\text{ L}^{-1}$, the presence of blowing snow particles does contribute significantly but it is important to consider that in this region MOR_BS overestimates the wind velocity which in turn increases the number of blowing snow particles. Blowing snow particles also play an important role in correctly estimating IWC, particularly in the region of high wind speed. However, some gaps still need to be filled in the ICNC and IWC plots. Lloyd et al. (2015) mentions four possible mechanisms that could increase the ICNC, namely surface hoar crystals, blowing snow, preactivated aerosol and riming on mountain surfaces. Even if the last two were considered less important, we point out that SNOWPACK does not consider riming but it does take into account vapor deposition on snow surfaces. In addition it is able to predict surface hoar (Stössel et al., 2010), which is therefore included in the saltation layer and, as a consequence, into the blowing snow particle counts. Lifting and transport of surface hoar crystals from the ground to the clouds, as well as blowing snow, are indeed considered important mechanisms for ICNC. Given the results in Sect. 3.2, it is appropriate to consider the effect of the primary ice production scheme to numerically model the correct ICNC. This is particularly true considering that the overall effect of an advanced PIP scheme is nearly similar to the effect of adding a SIP for breakup mechanisms. Each of the mechanisms for ICNC must be modeled or parametrized correctly, otherwise there is a risk of overestimation when all of them are considered at the same time.

Also shown in Fig. 7 is the influence of the newly implemented saltation scheme. The simulation MOR_BSorig represents the saltation scheme originally implemented in CRYOWRF v1.0.0 as boundary condition for the blowing snow equations. The new scheme implemented in MOR_BS, seems to better represent the measured data in most time windows considered. The

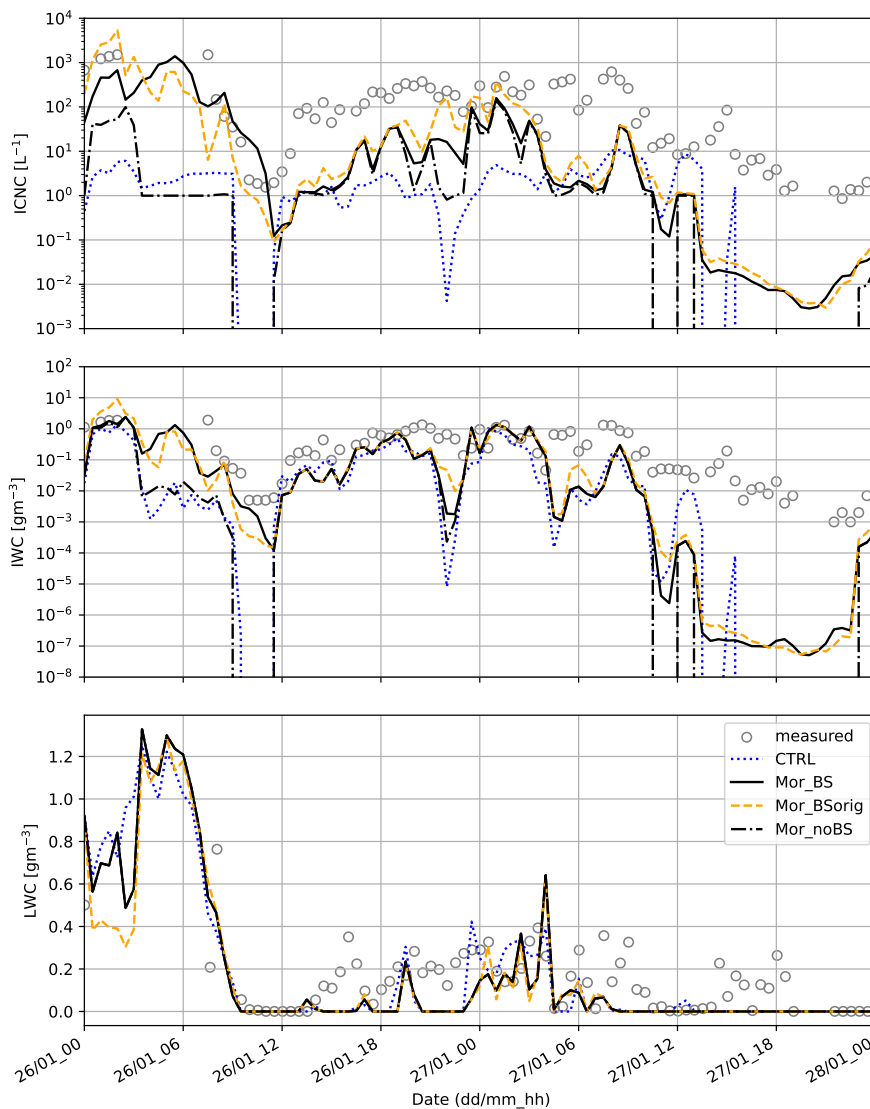


Figure 7. Analyzing the influence of SIP and blowing snow particles compared to the CTRL simulation. Plots show, from top to bottom, ice crystal number concentration, ice water concentration and liquid water concentration.

235 effect of the saltation scheme is non negligible, which demonstrates the importance of correctly parameterizing saltation for a proper lower boundary condition of the blowing snow equations.

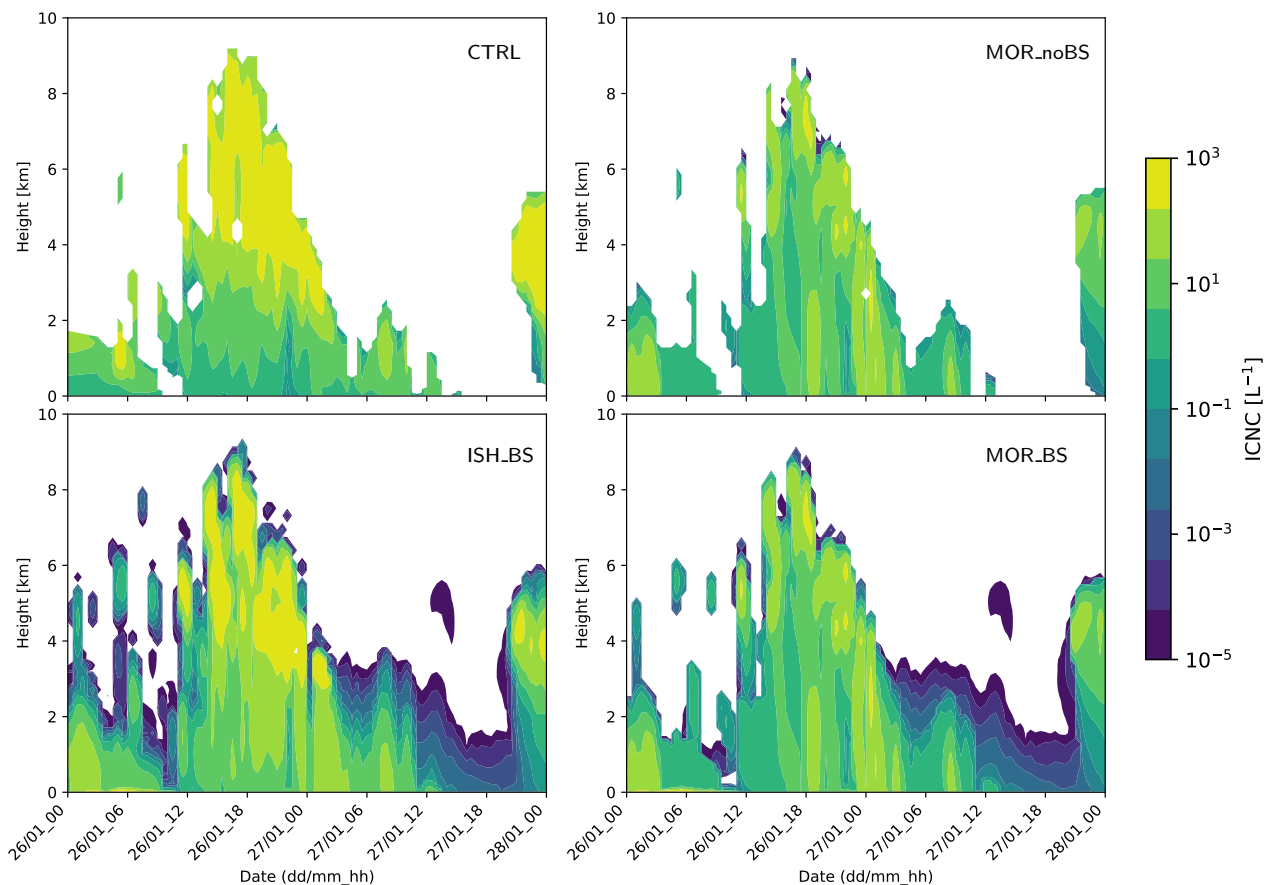


Figure 8. ICNC in the vertical direction over time. First row CTRL - MOR_noBS; second row ISH_BS - MOR_BS.

3.4 Blowing snow in the vertical direction

The temporal distribution of blowing snow particles in the vertical direction is shown through changes in ICNC based on the microphysics scheme and secondary ice production for the same time period considered. In Fig. 8, CTRL is first shown as
 240 reference on the top left corner, which is similar to the same case analyzed by Georgakaki et al. (2022) using WRF v4.0.1. The influence of the secondary ice production is demonstrated on the top right corner, where the blowing snow particles are not counted. Activating secondary ice production does modify the cloud microstructure, shifting the high concentration of particles visible in CTRL from high in the cloud (colored in yellow) closer to the surface, leading to a reduction in the vertical availability of LWC, a result also found in Georgakaki et al. (2024). The plot on the bottom right, MOR_BS, shows that small
 245 concentration of blowing snow particles reach high levels in the atmosphere. This is not surprising considering that during the MOSAiC expedition in the Arctic, Bergner et al. (2025) measured blowing snow heights that reached 145 m with winds at ~

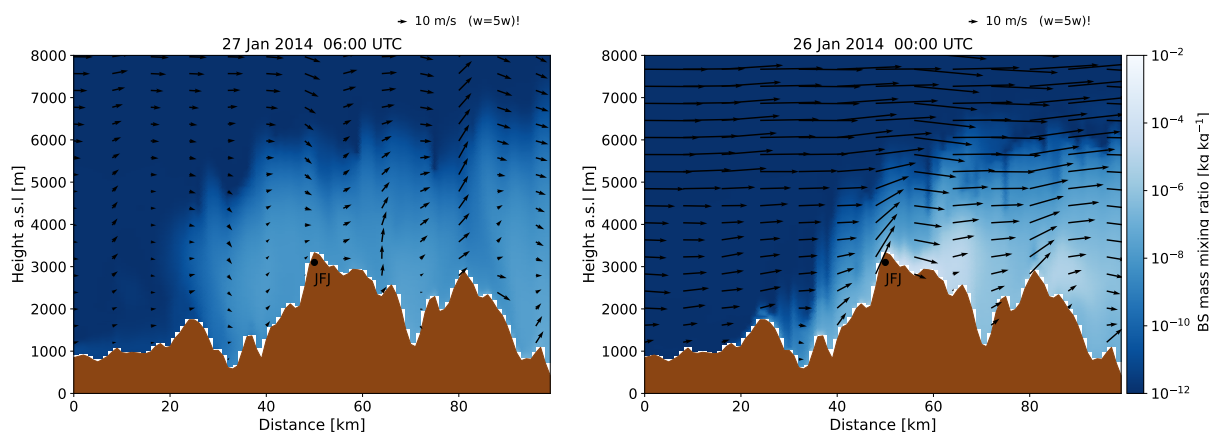


Figure 9. Comparing blowing snow mass mixing ratio in the cross section A-A' for low (left) or high (right) wind speed using MOR_BS. Vertical velocity components w are scaled five times for clarity.

10 m s⁻¹, without the influence of the strong updrafts generated by mountains. This suggests a possible interaction of BS with cloud microphysics which could affect precipitation events. Recall that with the equations now implemented in CRYOWRF, the only interaction with the cloud microphysics is through the water vapor source-sink term. None of the microphysical processes in MOR are currently implemented for blowing snow particles. The last case considered is the simulation ISH_BS, on the bottom left. The influence of the microphysics scheme is evident by the increase of particle concentration especially in the top part of the cloud. The influence of BS particles is also evident in the vertical direction.

The spatial redistribution of blowing snow particles in the vertical direction is plotted in Fig. 9 along the cross section A-A' shown in Fig. 1. The left image is the case of low wind speed of 27 January at 06:00 whereas the right image is the case with high wind speed of 26 January at 00:00. Black arrows show wind direction and magnitude along the cross section, with vertical velocities scaled by five times to better visualize their direction with respect to the horizontal flow. As expected, at high wind speed the blowing snow mixing ratio increases by several orders of magnitude. Strong winds also force the blowing snow particles closer to the highest peak of JFJ. Note that in the first 20 km the absence of blowing snow particles is caused by a low snow depth on the ground. The presence of three mountain peaks causes the flow above to form wavy patterns, particularly visible in the case of low wind speed. The strong updraft velocities on the windward side of JFJ followed by downdraft velocities on the leeward side help visualize the effects of erosion and deposition mechanisms that contribute to the redistribution of snow on mountain terrains. Both scenarios show that blowing snow particles reach high levels in the atmosphere potentially interacting with mixed-phased clouds typical of alpine regions.

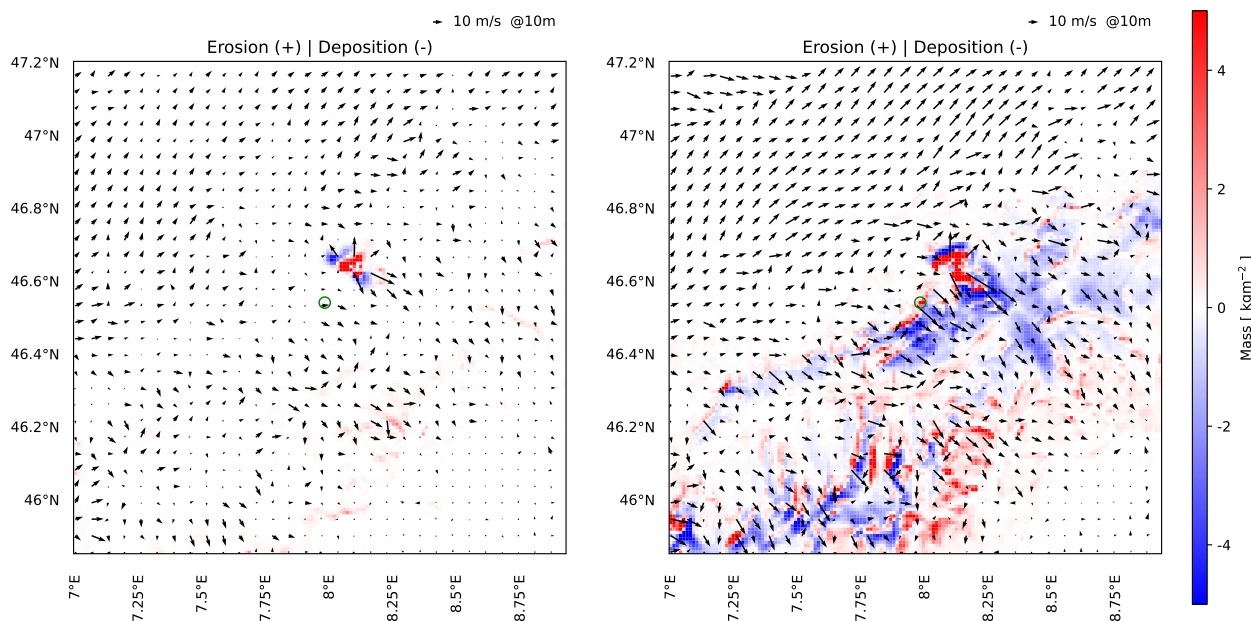


Figure 10. Cumulative erosion-deposition patterns for MOR_BS in 18 hours of low (left) and high (right) wind speed conditions. The green circle in the center shows the location of JFJ. Velocity vectors are plotted at 10 m. A color-blind version is provided in the supplementary material as Fig. S2 (left) and Fig. S3 (right).

3.5 Erosion and deposition patterns

265 The spatial distribution of blowing snow transport due to erosion and deposition is shown in Fig. 10. Values are cumulative in
 270 time for both plots. For the low speed case (left) the time considered starts from 27 January at 06:00 until 28 January at 00:00,
 whereas for the high speed case (right) the start is on 26 January at 00:00 until 26 January at 18:00. Black arrows show the
 horizontal velocity magnitude and direction at 10 m above the ground at the beginning of the relative time range. As expected,
 the higher the wind speed the more redistribution occurs. Comparing these results with the topography of the region (see Fig.
 1) shows that snow deposits more on the leeward sides of ridges and is more eroded on the windward side, following the pattern
 found by Mott et al. (2010) and Gerber et al. (2019) in their investigation of snow transport processes in the Swiss Alps near
 Davos. In particular, the region south-east of JFJ shows a marked deposition of snow, which is expected given the incoming
 north-westerly winds and the results plotted in Fig. 9. Snow can be easily transported horizontally for long distances due to the
 combination of vertical advection caused by the mountain ridges and strong horizontal winds above them.

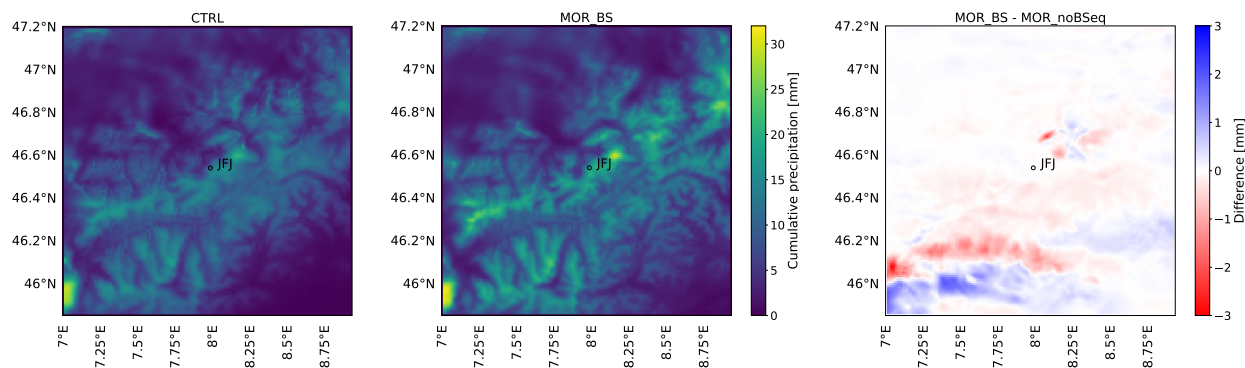


Figure 11. Cumulative precipitation computed for CTRL (left) and MOR_BS (center). Difference of cumulative precipitation with and without blowing snow equations (right). The black circle indicates the location of JFJ. A color-blind version is provided in the supplementary material as Fig. S4 (right).

275 Reynolds et al. (2024b) showed that coupling intermediate-complexity snow and atmospheric models can also be a valid approach for the estimation of preferential deposition and snow redistribution in alpine regions, particularly in regard to their lower computational costs.

3.6 Influence of blowing snow on precipitation

Based on the previous discussion, we here show the influence of the SIP and BS on precipitation, cumulated between 26
 280 January at 12:00 and 27 January at 02:30, which refers to the time range when JFJ is covered by clouds (see Fig. 8). Results from the CTRL simulation and MOR_BS are shown in Fig. 11 left and center, respectively. In addition, the right image shows the difference between MOR_BS and MOR_noBSeq, which was computed to better visualize the effect of adding blowing snow prognostic equations in the model. Recall that the MOR_BS includes both the effect of the SIP and BS. On the other hand, the MOR_noBSeq is a simulation in which the SIP is turned on but the blowing snow equations are completely turned
 285 off. Implementing a SIP mechanism based on breakup collision is here shown to affect also precipitation. The increase of precipitation caused by SIP can also be noticed comparing the top-left and top-right images of Fig. 8, where there is a strong decrease of ICNC in the high level of the cloud. This is particularly true at JFJ where the effect of blowing snow on precipitation is negligible (see right image). Notice that the increase of precipitation shown in MOR_BS due to the SIP is distributed across the entire mountain range of domain d03. On the contrary, the effect of blowing snow alone is concentrated on the high
 290 mountain range south of JFJ.

4 Conclusions

The primary focus of this paper is to support the hypothesis that blowing snow particles are important to be considered when trying to understand why the measured ice crystal number concentration are orders of magnitude higher than ice nucleating



particles. Neglecting blowing snow in atmospheric models will result in a strong disagreement between measured data and
295 numerical results. For the simulations, we use CRYOWRF in which an atmospheric model is coupled with an advanced land
surface model that represents snow on the ground and in the boundary layer with a high level of complexity. This is important,
since snow transport is governed both by wind speed and surface snow properties. The saltation scheme implemented in
CRYOWRF was also recently modified to better reproduce the necessary boundary conditions for the blowing snow equations
implemented in the model. Also included in the model is a secondary ice production mechanism based on collision breakup,
300 which is effective at temperatures here investigated. Measured data used for comparison of ice crystal number concentration
are taken from the CLAVE campaign performed at Jungfrauoch, in the Swiss Alps.

Results show that blowing snow is particularly relevant in filling the gap between measured and modeled ICNC at high
wind speeds. In addition, we show that, given the topography of the region, strong updraft winds can transport blowing snow
particles to high levels in the atmosphere, where they could potentially interact with cloud microphysical processes. We also
305 confirm the importance of adding secondary ice production mechanisms to improve the estimation of ice particles. Simulations
were run to show that advanced microphysical schemes, e.g. ISHMAEL, focused on better reproducing primary ice production,
are also important to consider. When blowing snow particles are included in these schemes, the overall effect on the results
is comparable to a simulation with a standard microphysics scheme that includes secondary ice production. To conclude our
investigation we show how modeling blowing snow can give valuable information on snow redistribution through erosion-
310 deposition, and precipitation.

Future work will consider adding SIP mechanisms into the ISHMAEL scheme, for example the breakup mechanism imple-
mented here. In addition, in the context of collisional breakup, blowing snow particles could be added as source of collisions
with other icy hydrometeors whereas in the context of cloud microphysics, blowing snow particles should also be allowed to
interact with other hydrometeors. If well resolved, both snow transport and precipitation can be accurate forcing terms for the
315 land surface model SNOWPACK, originally designed for avalanche forecasting. Additional tests must be performed to validate
CRYOWRF by comparing precipitation and snow transport results with measured data.

Code availability. CRYOWRF v1.2.2 is publicly available via GNU GPL v3 License at <https://gitlabext.wsl.ch/atmospheric-models/CRYOWRF>.

Data availability. Data from the numerical simulations and observations presented in this paper are available on the EnviDat portal at
<https://www.doi.org/10.16904/envodat.754> (Viaro et al., 2026), where the input files used to set up the numerical models are also present.

320 Please use the following link during the review process: <https://www.envodat.ch/#/review/f4c1ffd0-0956-42dd-94a4-3ddab1a1d355>



Author contributions. SV ran the simulations, prepared post-processing scripts for analyzing numerical data, and helped updating CRYOWRF to v1.2.2. AS developed the new saltation method in CRYOWRF v.1.2.2. ET designed the structure of the new gitLab repository for CRYOWRF v.1.2.2. ML guided the project. All four authors contributed to writing the paper.

Competing interests. The contact author states that none of the authors have any competing interests.

325 *Disclaimer.* Publisher’s note: Copernicus Publications remains neutral with regard to jurisdictional claims in published maps and institutional affiliations.

Acknowledgements. We kindly thank the Swiss National Supercomputer Center (CSCS) for providing the computational resources needed through project s1329. Our main funding has been provided by the Swiss National Science Foundation for the project “Large-Scale Influence of Small-Scale Snow Processes”, grant number 215406. We would like to thank Paraskevi Georgakaki for giving us access to their results
330 for comparison with our simulations. Finally we are very grateful to the open-source software community and AI tools such as Gemini, ChatGPT and Claude.



References

- Baltensperger, U., Schwikowski, M., Jost, D., Nyeki, S., Gäggeler, H., and Poulida, O.: Scavenging of atmospheric constituents in mixed phase clouds at the high-alpine site Jungfrauoch part I: Basic concept and aerosol scavenging by clouds, *Atmospheric Environment*, 32, 3975–3983, [https://doi.org/10.1016/S1352-2310\(98\)00051-X](https://doi.org/10.1016/S1352-2310(98)00051-X), 1998.
- 335
- Beaumet, J., Ménégos, M., Morin, S., Gallée, H., Fettweis, X., Six, D., Vincent, C., Wilhelm, B., and Anquetin, S.: Twentieth century temperature and snow cover changes in the French Alps, *Regional Environmental Change*, 21, 114, <https://doi.org/10.1007/s10113-021-01830-x>, 2021.
- Bergner, N., Heutte, B., Beck, I., Pernov, J. B., Angot, H., Arnold, S. R., Boyer, M., Creamean, J. M., Engelmann, R., Frey, M. M., et al.: Characteristics and effects of aerosols during blowing snow events in the central Arctic, *Elem Sci Anth*, 13, 00047, <https://doi.org/10.1525/elementa.2024.00047>, 2025.
- 340
- Field, P. and Heymsfield, A.: Importance of snow to global precipitation, *Geophysical Research Letters*, 42, 9512–9520, <https://doi.org/10.1002/2015GL065497>, 2015.
- Geerts, B., Pokharel, B., and Kristovich, D. A.: Blowing snow as a natural glaciogenic cloud seeding mechanism, *Monthly Weather Review*, 143, 5017–5033, <https://doi.org/10.1175/MWR-D-15-0241.1>, 2015.
- 345
- Georgakaki, P., Sotiropoulou, G., Vignon, É., Billault-Roux, A.-C., Berne, A., and Nenes, A.: Secondary ice production processes in winter-time alpine mixed-phase clouds, *Atmospheric Chemistry and Physics*, 22, 1965–1988, <https://doi.org/10.5194/acp-22-1965-2022>, 2022.
- Georgakaki, P., Billault-Roux, A.-C., Foskinis, R., Gao, K., Sotiropoulou, G., Gini, M., Takahama, S., Eleftheriadis, K., Papayannis, A., Berne, A., et al.: Unraveling ice multiplication in winter orographic clouds via in-situ observations, remote sensing and modeling, *npj Climate and Atmospheric Science*, 7, 145, <https://doi.org/10.1038/s41612-024-00671-9>, 2024.
- 350
- Gerber, F., Mott, R., and Lehning, M.: The importance of near-surface winter precipitation processes in complex alpine terrain, *Journal of Hydrometeorology*, 20, 177–196, <https://doi.org/10.1175/JHM-D-18-0055.1>, 2019.
- Grazioli, J., Lloyd, G., Panziera, L., Hoyle, C. R., Connolly, P. J., Henneberger, J., and Berne, A.: Polarimetric radar and in situ observations of riming and snowfall microphysics during CLACE 2014, *Atmospheric Chemistry and Physics*, 15, 13 787–13 802, <https://doi.org/10.5194/acp-15-13787-2015>, 2015.
- 355
- Hersbach, H., Bell, B., Berrisford, P., Hirahara, S., Horányi, A., Muñoz-Sabater, J., Nicolas, J., Peubey, C., Radu, R., Schepers, D., et al.: The ERA5 global reanalysis, *Quarterly journal of the royal meteorological society*, 146, 1999–2049, <https://doi.org/10.1002/qj.3803>, 2020.
- Hoarau, T., Pinty, J.-P., and Barthe, C.: A representation of the collisional ice break-up process in the two-moment microphysics LIMA v1.0 scheme of Meso-NH, *Geoscientific Model Development*, 11, 4269–4289, <https://doi.org/10.5194/gmd-11-4269-2018>, 2018.
- 360
- Jensen, A. A., Harrington, J. Y., Morrison, H., and Milbrandt, J. A.: Predicting ice shape evolution in a bulk microphysics model, *Journal of the Atmospheric Sciences*, 74, 2081–2104, <https://doi.org/10.1175/JAS-D-16-0350.1>, 2017.
- Korolev, A., DeMott, P. J., Heckman, I., Wolde, M., Williams, E., Smalley, D. J., and Donovan, M. F.: Observation of secondary ice production in clouds at low temperatures, *Atmospheric Chemistry and Physics*, 22, 13 103–13 113, <https://doi.org/10.5194/acp-22-13103-2022>, 2022.
- Lehning, M. and Fierz, C.: Assessment of snow transport in avalanche terrain, *Cold Regions Science and Technology*, 51, 240–252, <https://doi.org/10.1016/j.coldregions.2007.05.012>, 2008.
- 365
- Lehning, M., Bartelt, P., Brown, B., Russi, T., Stöckli, U., and Zimmerli, M.: SNOWPACK model calculations for avalanche warning based upon a new network of weather and snow stations, *Cold Regions Science and Technology*, 30, 145–157, [https://doi.org/10.1016/S0165-232X\(99\)00022-1](https://doi.org/10.1016/S0165-232X(99)00022-1), 1999.



- Lehning, M., Löwe, H., Ryser, M., and Raderschall, N.: Inhomogeneous precipitation distribution and snow transport in steep terrain, *Water Resources Research*, 44, <https://doi.org/10.1029/2007WR006545>, 2008.
- Lloyd, G., Choullarton, T. W., Bower, K. N., Gallagher, M. W., Connolly, P. J., Flynn, M., Farrington, R., Crosier, J., Schlenczek, O., Fugal, J., et al.: The origins of ice crystals measured in mixed-phase clouds at the high-alpine site Jungfraujoch, *Atmospheric Chemistry and Physics*, 15, 12 953–12 969, <https://doi.org/10.5194/acp-15-12953-2015>, 2015.
- Mellor, M.: Blowing snow, Tech. rep., US Army Materiel Command, Cold Regions Research & Engineering Laboratory, 1965.
- 375 Melo, D. B., Sharma, V., Comola, F., Sigmund, A., and Lehning, M.: Modeling snow saltation: the effect of grain size and interparticle cohesion, *Journal of Geophysical Research: Atmospheres*, 127, e2021JD035 260, <https://doi.org/10.1029/2021JD035260>, 2022.
- Melo, D. B., Sigmund, A., and Lehning, M.: Understanding snow saltation parameterizations: lessons from theory, experiments and numerical simulations, *The Cryosphere*, 18, 1287–1313, <https://doi.org/10.5194/tc-18-1287-2024>, 2024.
- Mignani, C., Creamean, J. M., Zimmermann, L., Alewell, C., and Conen, F.: New type of evidence for secondary ice formation at around-15°C in mixed-phase clouds, *Atmospheric Chemistry and Physics*, 19, 877–886, <https://doi.org/10.5194/acp-19-877-2019>, 2019.
- 380 Morrison, H., Thompson, G., and Tatarskii, V.: Impact of cloud microphysics on the development of trailing stratiform precipitation in a simulated squall line: Comparison of one-and two-moment schemes, *Monthly weather review*, 137, 991–1007, <https://doi.org/10.1175/2008MWR2556.1>, 2009.
- Mott, R., Schirmer, M., Bavay, M., Grünewald, T., and Lehning, M.: Understanding snow-transport processes shaping the mountain snow-cover, *The Cryosphere*, 4, 545–559, <https://doi.org/10.5194/tc-4-545-2010>, 2010.
- 385 Mott, R., Scipión, D., Schneebeli, M., Dawes, N., Berne, A., and Lehning, M.: Orographic effects on snow deposition patterns in mountainous terrain, *Journal of Geophysical Research: Atmospheres*, 119, 1419–1439, <https://doi.org/10.1002/2013JD019880>, 2014.
- Nishimura, K. and Hunt, J.: Saltation and incipient suspension above a flat particle bed below a turbulent boundary layer, *Journal of Fluid Mechanics*, 417, 77–102, <https://doi.org/10.1017/S0022112000001014>, 2000.
- 390 Nishimura, K. and Nemoto, M.: Blowing snow at Mizuho station, Antarctica, *Philosophical Transactions of the Royal Society A: Mathematical, Physical and Engineering Sciences*, 363, 1647–1662, <https://doi.org/10.1098/rsta.2005.1599>, 2005.
- Nishimura, K., Yokoyama, C., Ito, Y., Nemoto, M., Naaim-Bouvet, F., Bellot, H., and Fujita, K.: Snow particle speeds in drifting snow, *Journal of Geophysical Research: Atmospheres*, 119, 9901–9913, <https://doi.org/10.1002/2014JD021686>, 2014.
- Niu, G.-Y., Yang, Z.-L., Mitchell, K. E., Chen, F., Ek, M. B., Barlage, M., Kumar, A., Manning, K., Niyogi, D., Rosero, E., et al.: The community Noah land surface model with multiparameterization options (Noah-MP): 1. Model description and evaluation with local-scale measurements, *Journal of Geophysical Research: Atmospheres*, 116, <https://doi.org/10.1029/2010JD015139>, 2011.
- 395 Pomeroy, J. and Male, D.: Steady-state suspension of snow, *Journal of hydrology*, 136, 275–301, [https://doi.org/10.1016/0022-1694\(92\)90015-N](https://doi.org/10.1016/0022-1694(92)90015-N), 1992.
- Reynolds, D., Haugeneder, M., Lehning, M., and Mott, R.: Intermediate complexity atmospheric modeling in complex terrain: is it right?, *Frontiers in Earth Science*, 12, 1388 416, <https://doi.org/10.3389/feart.2024.1388416>, 2024a.
- 400 Reynolds, D., Quéno, L., Lehning, M., Jafari, M., Berg, J., Jonas, T., Haugeneder, M., and Mott, R.: Seasonal snow–atmosphere modeling: let’s do it, *The Cryosphere*, 18, 4315–4333, <https://doi.org/10.5194/tc-18-4315-2024>, 2024b.
- Roe, G. H.: Orographic precipitation, *Annu. Rev. Earth Planet. Sci.*, 33, 645–671, <https://doi.org/10.1146/annurev.earth.33.092203.122541>, 2005.



- 405 Saigger, M., Sauter, T., Schmid, C., Collier, E., Goger, B., Kaser, G., Prinz, R., Voordendag, A., and Mölg, T.: A drifting and blowing snow scheme in the weather research and forecasting model, *Journal of Advances in Modeling Earth Systems*, 16, e2023MS004007, <https://doi.org/10.1029/2023MS004007>, 2024.
- Schmidt, R.: Properties of blowing snow, *Reviews of Geophysics*, 20, 39–44, <https://doi.org/10.1029/RG020i001p00039>, 1982a.
- Schmidt, R.: Vertical profiles of wind speed, snow concentration, and humidity in blowing snow, *Boundary-Layer Meteorology*, 23, 223–246, <https://doi.org/10.1007/BF00123299>, 1982b.
- 410 Sharma, V., Gerber, F., and Lehning, M.: Introducing CRYOWRF v1.0: multiscale atmospheric flow simulations with advanced snow cover modelling, *Geoscientific Model Development*, 16, 719–749, <https://doi.org/10.5194/gmd-16-719-2023>, 2023.
- Sigmund, A., Melo, D., Dujardin, J., Nishimura, K., and Lehning, M.: Parameterizing snow sublimation in conditions of drifting and blowing snow, *Journal of Advances in Modeling Earth Systems*, 17, e2024MS004332, <https://doi.org/10.1029/2024MS004332>, 2025.
- 415 Sotiropoulou, G., Vignon, É., Young, G., Morrison, H., O’Shea, S. J., Lachlan-Cope, T., Berne, A., and Nenes, A.: Secondary ice production in summer clouds over the Antarctic coast: an underappreciated process in atmospheric models, *Atmospheric Chemistry and Physics Discussions*, 2020, 1–30, <https://doi.org/10.5194/acp-21-755-2021>, 2020.
- Sotiropoulou, G., Lewinschal, A., Georgakaki, P., Phillips, V. T., Patade, S., Ekman, A. M., and Nenes, A.: Sensitivity of Arctic clouds to ice microphysical processes in the NorESM2 climate model, *Journal of Climate*, 37, 4275–4290, <https://doi.org/10.1175/JCLI-D-22-0458.1>, 2024.
- 420 Stössel, F., Guala, M., Fierz, C., Manes, C., and Lehning, M.: Micrometeorological and morphological observations of surface hoar dynamics on a mountain snow cover, *Water Resources Research*, 46, <https://doi.org/10.1029/2009WR008198>, 2010.
- Takahashi, T. and Nagao, Y.: Possible high ice particle production during Graupel-Graupel collisions., *Journal of the atmospheric sciences*, 52, [https://doi.org/10.1175/1520-0469\(1995\)052<4523:PHIPPD>2.0.CO;2](https://doi.org/10.1175/1520-0469(1995)052<4523:PHIPPD>2.0.CO;2), 1995.
- 425 Vali, G.: Nucleation terminology, *Bulletin of the American Meteorological Society*, 66, 1426–1427, 1985.
- van Dalum, C. T., van de Berg, W. J., van den Broeke, M. R., and van Tiggelen, M.: The surface mass balance and near-surface climate of the Antarctic ice sheet in RACMO2. 4p1, *The Cryosphere*, 19, 4061–4090, <https://doi.org/10.5194/tc-19-4061-2025>, 2025.
- Viaro, S., Sigmund, A., Thomas, E., and Lehning, M.: The importance of alpine blowing snow for cloud processes, *Envidat [data set]*, <https://doi.org/10.16904/envidat.754>, 2026.
- 430 Vionnet, V., Martin, E., Masson, V., Guyomarc’h, G., Naaim-Bouvet, F., Prokop, A., Durand, Y., and Lac, C.: Simulation of wind-induced snow transport and sublimation in alpine terrain using a fully coupled snowpack/atmosphere model, *The Cryosphere*, 8, 395–415, <https://doi.org/10.5194/tc-8-395-2014>, 2014.
- Yang, Z.-L., Niu, G.-Y., Mitchell, K. E., Chen, F., Ek, M. B., Barlage, M., Longuevergne, L., Manning, K., Niyogi, D., Tewari, M., et al.: The community Noah land surface model with multiparameterization options (Noah-MP): 2. Evaluation over global river basins, *Journal of Geophysical Research: Atmospheres*, 116, <https://doi.org/10.1029/2010JD015140>, 2011.
- 435